ELSEVIER

Journal of Molecular Catalysis A: Chemical 177 (2001) 149–164

JOURNAL OF MOLECULAR CATALYSIS A: CHEMICAL

www.elsevier.com/locate/molcata

2-Ethyl-9,10-anthraquinone hydrogenation over Pd/polymers Effect of polymers–Pd(II) chlorocomplexes interactions

A. Drelinkiewicz [a,*], M. Hasik [b]

[a] *Department of Chemistry, Jagiellonian University, Ingardena 3, 30-060 Kraków, Poland*

[b] *Department of Materials Science and Ceramics, Academy of Mining and Metallurgy, Al. Mickiewicza 30, 30-059 Kraków, Poland*

Received 31 October 2000; received in revised form 27 December 2000; accepted 5 June 2001

Abstract

Two polymers, namely poly(4-vinylpyridine) (PVP) and polyaniline (PANI), were used as the supports for palladium catalysts acting in 2-ethyl-9,10-anthraquinone (EAQ) hydrogenation, a key step in the industrial production of H_2O_2. The nature of PVP and PANI interactions with various chlorocomplexes of Pd(II) coexisting in $PdCl_2$–H_2O–HCl solutions was studied using IR (mid-IR, far-IR), UV–Vis and XPS spectroscopies. It was found that the type of interactions involving nitrogen atoms of the polymers depended mainly on the acidity of $PdCl_2$ solution. Protonation of polymers (via acid–base reactions) as well as coordination of Pd^{2+} ions by nitrogen atoms of the polymers took place in highly acidic $PdCl_2$ solution (2 M HCl) containing predominantly anionic $[PdCl_4]^{2-}$, $[PdCl_3(H_2O)]^-$ complexes (series A of experiments). In the weakly acidic $PdCl_2$ solutions (0.66×10^{-3} M HCl) (series B of experiments) containing predominantly electrically neutral $[PdCl_2(H_2O)_2]$ complexes, hydrolysis of the complex proceeded as the main process resulting in precipitation of palladium oxide on PVP. In the case of PANI in solution B, the redox mechanism was involved resulting in the reduction of some Pd^{2+} to Pd^0 accompanied by partial oxidation of the polymer chain. As a consequence of various mechanisms of polymers reactions with Pd^{2+} ions, surface morphology of the final catalysts, characterized by XRD and SEM methods, was different. It was found that dispersion of palladium in Pd/PVP and Pd/PANI catalysts (1–10 wt.% Pd) influenced the course of EAQ hydrogenation. The presence of large palladium particles promoted reactions leading to the formation of the so-termed "degradation products" not capable of hydrogen peroxide formation. Pd/PVP catalysts (series B) exhibited higher activity. Selectivity of EAQ hydrogenation in their presence was better than that seen for Pd/PANI catalysts.

Keywords: Polyaniline; Poly(4-vinylpyridine); Palladium catalysts; 2-Ethyl-9,10-anthraquinone hydrogenation

1. Introduction

In recent years, the application of polymer-immobilized transition metal catalysts has been extensively studied. However, more often they are studied in homogeneous conditions of catalytic processes. Therefore, it seems interesting to investigate the possibility of using polymers as the supports for Pd catalysts acting in heterogeneous conditions. The present work deals with poly(4-vinylpyridine) (PVP)- and polyaniline (PANI)-supported palladium catalysts. Nitrogen atoms existing in the structure of both polymers used (Scheme 1) constitute potential sites for polymer–Pd(II) chlorocomplexes interactions.

Abbreviations: EAQ, 2-ethyl-9,10-anthraquinone; $EAQH_2$, 2-ethyl-9,10-anthrahydroquinone; H_4EAQ, 2-ethyltetrahydro-9,10-anthraquinone; H_4EAQH_2, 2-ethyl-9,10-anthrahydroquinone

* Corresponding author.

1381-1169/01/$ – see front matter
PII: S1381-1169(01)00315-6

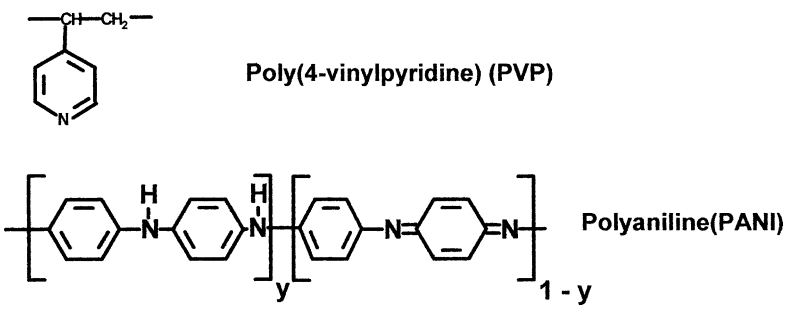

Scheme 1.

PVP–Pd^{2+} system is discussed in a number of papers [1–5]. They show that nitrogen atoms in PVP (polymer in the solid state or dissolved) form complexes with Pd^{2+} (water–alcohol solutions of K_2PdCl_4 or $PdCl_2$). Catalytic activity of Pd/PVP in the hydrogenation of C_3–C_5 unsaturated alcohols has been studied [2,3]. It has also been shown that nitrogen atoms present in PANI structure (amine (–NH–) and imine (=N–) groups) are able to coordinate Ag^+ [6], Cu^{2+} [7] and Pd^{2+} [8] ions in the electrochemically doped polymer. The information of the use of PANI in catalytic systems is limited, though this polymer has been used as the support for Pd and Pt catalysts exhibiting interesting behaviour in hydrogenation of unsaturated hydrocarbons [9] and nitrobenzene [10].

The aim of this research was to investigate catalytic properties of Pd/PVP and Pd/PANI systems depending on the method of their preparation as well as on their physico-chemical characteristics. In particular, the following problems have been studied and are discussed in the paper:

- Interactions between polymers and various chlorocomplexes of Pd^{2+} present in the $PdCl_2$ solutions of various acidity. It was interesting to correlate the nature of these interactions (protonation, coordination, oxidation–reduction processes) with the type of Pd^{2+} complexes.
- Influence of the type of Pd^{2+}–polymers species formed on the surface morphology and especially on Pd^0 dispersion obtained after reduction of the samples.
- Influence of polymer type as well as the dispersion of Pd^0 on the catalytic properties of Pd/PVP and Pd/PANI samples.

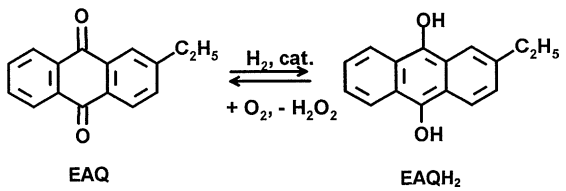

Scheme 2.

As a model reaction for testing the catalytic ability of the systems studied, liquid-phase hydrogenation of 2-ethyl-9,10-anthraquinone (EAQ) (Scheme 2), the main reaction of H_2O_2 production in the anthraquinone method [11] has been chosen. In the hydrogenation stage of the anthraquinone method, palladium catalysts supported on Al_2O_3, SiO_2 and silica–alumina are commonly applied [11,12]. However, according to patent literature [13], also Pd^{2+}–polyethyleneimine systems have recently been successfully applied.

In this paper, the most important effects from the investigations published earlier in a number of our papers as well as some new results, especially concerning the physico-chemical and catalytic properties of Pd/PVP systems, are presented.

2. Experimental

2.1. Materials

PANI powder (BET surface area $46\,m^2/g$) was synthesized according to a standard procedure [14] by oxidation of aniline with $(NH_4)_2S_2O_8$ in hydrochloric acid followed by deprotonation with aqueous ammo-

nia. PVP powder (BET surface area 17 m^2/g) was purchased from Aldrich.

For the catalysts preparation, two aqueous solutions of $PdCl_2$ (A and B) strongly differing in the concentration of HCl were used. In both solutions, $PdCl_2$ concentration was the same and equal to 2.3×10^{-3} mol/dm^3. In solution A, the concentration of HCl was high (2 mol/dm^3) whereas in solution B it was as low as 0.66×10^{-3} mol/dm^3.

PANI or PVP powders were exposed at room temperature to the solution of $PdCl_2$ (A or B). The suspension was stirred until the total disappearance of Pd^{2+} ions in the solution (controlled by colorimetric method). The appropriate volume of the solution to give 1–10 wt.% of Pd in the final sample was used. After palladium sorption was complete (~96 h), the samples were filtered, washed with water until the Cl^- ions were eliminated and dried for 2 h at 110°C. In the case of PVP-series A experiments, the sorption of Pd^{2+} was complete after 30 min.

Colorimetric method based on the reaction between palladium ions and KI leading to the formation of $[PdI_4]^{2-}$ complexes [15] was used to control the completeness of Pd^{2+} sorption on polymers and to determine the content of Pd^{2+} in the Pd/PANI samples [16]. The content of Pd^{2+} was determined in the pristine Pd/PANI samples of series B and in Pd/PANI samples of series A after their reduction with NaH_2PO_2. It should be noted that the results obtained analytically are in accordance with those obtained by XPS method [17].

2.2. Characterization methods

FTIR spectroscopic studies in the middle infrared range (MIR) were carried out using a BioRad FTS 60v spectrometer and a standard KBr pellets technique. Studies in the far infrared range (FIR) were performed on a BioRad FT60 spectrometer in polyethylene pellets.

XPS spectra were recorded on a VSW Manchaster (model 100) spectrometer using Mg Kα radiation. The analyses were referenced to the graphite C 1s band (286.4 eV). UV–Vis spectra were recorded using a Perkin-Elmer Lambda 2 spectrophotometer. XRD studies were carried out using a HZG-4 diffractometer with Cu Kα radiation. Surface morphology of the catalysts was investigated by means of a scanning electron microscope (Philips XL-30) equipped with an X-ray microprobe enabling to carry out elemental (Pd, Cl) distribution studies (spot, surface, line profiles).

2.3. Catalytic experiments

EAQ hydrogenation was carried out under stirred batch reactor conditions at constant atmospheric pressure of hydrogen, temperature of 64°C using a mixture of xylene–octanol-2 (1:1 volume ratio) as the solvent [18]. The course of hydrogenation was followed by measuring the volume of hydrogen consumed as a function of reaction time. During the reaction, the samples of the solution were taken from the reactor, oxidized with air and the amount of H_2O_2 formed was determined by titration (using $KMnO_4$). The concentration of EAQ and H_4EAQ (2-ethyltetrahydro-9,10-anthraquinone) in the oxidized solution was determined by HPLC method [18,19]. Since the oxidation of $EAQH_2$ (2-ethyl-9,10-anthrahydroquinone) and H_4EAQH_2 (2-ethyl-9,10-anthrahydroquinone) is rapid and quantitative, it was assumed that the number of moles of $EAQH_2$ and H_4EAQH_2 in the hydrogenated solution was equal to the number of moles of EAQ and H_4EAQ determined by HPLC analysis.

Two series of hydrogenation experiments were carried out. In the first one 10 cm^3 of EAQ solution (20 g/dm^3) and 0.07 g of catalyst, and in the second one 40 cm^3 of the same EAQ solution and 0.2 g of catalyst were used. In the former case the activity of catalysts while in the latter the selectivity of hydrogenation were determined.

3. Results and discussion

3.1. Interactions between chlorocomplexes of Pd(II) and polymers

In the $PdCl_2$–H_2O–HCl solutions various Pd^{2+} chlorocomplexes may coexist. The concentration of individual species depends mainly on HCl content. The composition of $PdCl_2$ solutions (A and B) used in the present studies was selected based on the literature data [20,21] as well as on our own UV–Vis experiments [22]. The aim was to have two solutions A and B strongly differing in the type of dominating Pd^{2+} complexes.

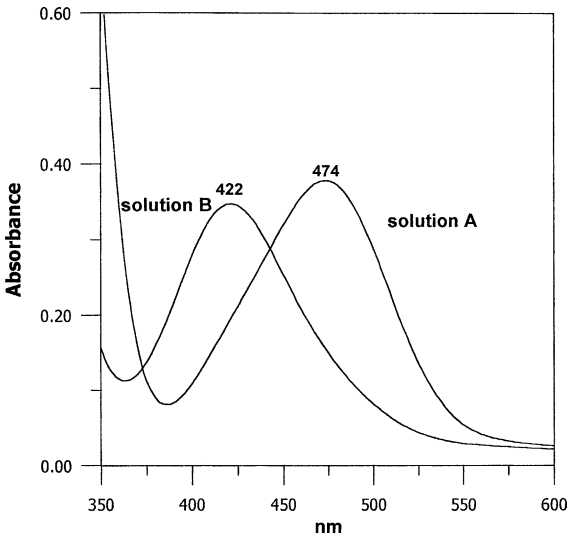

Fig. 1. UV–Vis spectra of $PdCl_2$ solutions used in the experiments ($c_{PdCl_2} = 2.3 \times 10^{-3}$ mol/dm^3).

In the $PdCl_2$ solution of very low acidity (HCl concentration 0.66×10^{-3} mol/dm^3) corresponding to series B, electrically neutral species $[PdCl_2(H_2O)_2]$ (about 60%) are the dominating ones. The content of chlorocomplexes in the $PdCl_2$ solution grows with the increase of HCl concentration and at HCl concentration as high as 2 mol/dm^3 (solution A of the experiments) anionic complexes, i.e. $[PdCl_4]^{2-}$ and $[PdCl_3(H_2O)]^-$, become dominant [20]. UV–Vis spectra registered for the solutions A and B have confirmed such composition (Fig. 1). In solution A, the maximum absorption at 474 nm has indicated the predominant presence of $[PdCl_4]^{2-}$ while in solution B this maximum has appeared at 422 nm which corresponds to the dominant presence of $[PdCl_2(H_2O)_2]$ [21].

Hence, interactions between the polymers used and palladium(II) chlorocomplexes involved mainly anionic, i.e. $[PdCl_4]^{2-}$ and $[PdCl_3(H_2O)]^-$, complexes in solution A and electrically neutral, i.e. $[PdCl_2(H_2O)_2]$ complexes in solution B.

For the sake of clarity, the results concerning the interactions between chlorocomplexes of Pd^{2+} ions and polymers will be discussed in separate chapters devoted to PVP and PANI.

3.1.1. PVP

The results of spectroscopic investigations (IR, Raman, UV–Vis and XPS) show that nature of PVP–Pd^{2+} interactions strongly depends on the type of palladium complexes dominating in the $PdCl_2$ solutions (A or B) used. Changes in the polymer structure resulting from these interactions have been more evidently observed in the MIR, whereas changes in the coordination sphere of palladium complexes in the FIR similarly to the case of transition metal–pyridine (Py) systems. In these systems, formation of Py*HCl salt (e.g. $(PyH)_2CoCl_4$) or Py–MeX_N bond (e.g. $MnPy_2Cl_2$) has been established using IR method [23].

In the solution of high acidity (type A) containing predominantly anionic $[PdCl_4]^{2-}$, $[PdCl_3(H_2O)]^-$ complexes, the formation of PVP salts (via protonation reaction) and coordination of Pd^{2+} ions by nitrogen atoms of PVP proceeds [24]. In FIR spectra of samples A, the bands at 340 cm^{-1} corresponding to Pd–Cl as well as at 280 cm^{-1} characteristic of Pd–N vibrations are seen (Fig. 2). The intensity of both bands grows as the content of palladium in the samples increases. The band at 280 cm^{-1} is visible even in the spectrum of the sample containing as little as 1 wt.% Pd (Fig. 3). Similar bands have been observed when alcohol solutions of PVP and K_2PdCl_4 were mixed [1,2]. The bands have been assigned to the formation of *trans*-complexes in which palladium ions are incorporated between the polymer chains and in consequence coordinated by the nitrogen atoms of two neighbouring polymer chains [1,2]. This may be

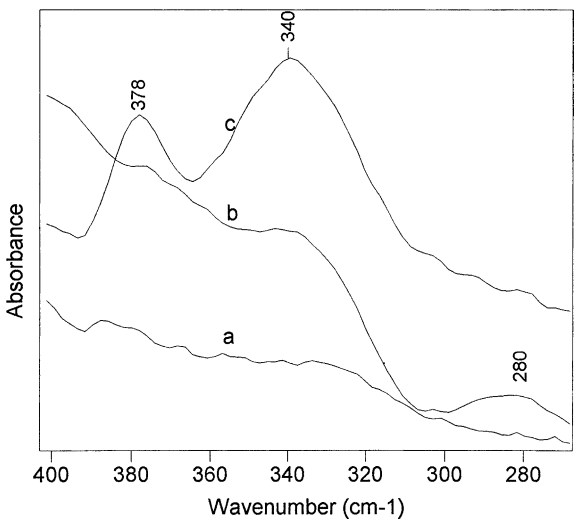

Fig. 2. FIR spectra of: (a) PVP; (b) PVP–Pd^{2+} prepared in solution A (4% Pd); (c) PVP–Pd^{2+} prepared in solution B (5.8% Pd).

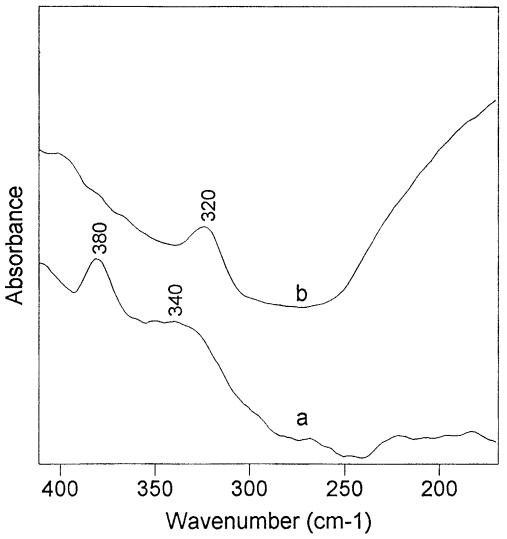

Fig. 3. FIR spectra of the samples PVP–Pd: (a) PVP–Pd prepared in solution A containing 1 wt.% Pd; (b) PVP–Pd prepared in solution B (4.14% Pd) treated with 2 M HCl.

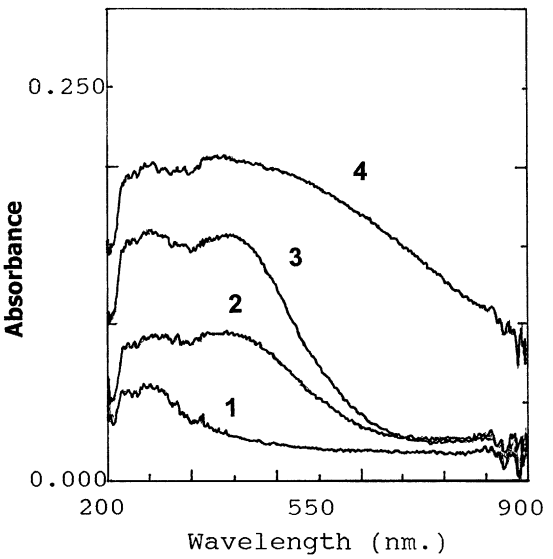

Fig. 4. UV–Vis reflection spectra of Pd/PVP: (1) PVP; (2) sample of type A containing 2% Pd; (3) sample of type A containing 4% Pd; (4) sample of type B containing 4.14% Pd.

the case also in the samples of type A. However, as MIR spectra of samples A show the protonation of the polymer proceeds simultaneously with the coordination reaction. Instead of the band at 1596 cm^{-1} due to C=N stretching vibrations present in the spectrum of starting PVP, in the spectra of samples A, a new band and 1635 cm^{-1} with a shoulder at 1612 cm^{-1} are observed [24]. According to Karklin et al. [2] and Sokolski et al. [3], the band at 1635 cm^{-1} corresponds to the HCl–protonated polymer while the shoulder at 1612 cm^{-1} may be attributed to PVP–Pd^{2+} coordination bond. In the UV–Vis spectra of the solid yellow samples of type A, broad bands in the region 380–410 nm have been detected (Fig. 4). It should be observed that the band characteristic of $[PdCl_4]^{2-}$ ions appear at 470 nm [21]. When some of Cl^- ligands in $[PdCl_4]^{2-}$ are substituted by the molecules of H_2O or nitrogen-containing ligands, this band shift to lower wavelengths and in $[Pd(H_2O)_4]^{2+}$ it appears at 420 nm while in $[Pd(NH_3)_4]^{2+}$ at 295 nm [21]. Hence, in solution of high acidity, both processes, protonation and coordination, take place simultaneously.

In the $PdCl_2$ solution of low acidity of type B, electrically neutral $[PdCl_2(H_2O)_2]$ complexes are the dominating species. In the MIR spectra, except a very weak band at 1635 cm^{-1}, no changes with respect to the spectrum of the starting PVP are observed. FIR spectra show the intensive band at 340 cm^{-1} characteristic of Pd–Cl vibrations and a new one at 378 cm^{-1} (Fig. 2). Using other methods (UV–Vis, XPS), it has been established that in the system of type B hydrated palladium oxide or hydroxide type compounds precipitate on the polymer grains. It cannot be excluded that the band at 378 cm^{-1} corresponds to these compounds because upon treatment of brown-coloured sample B with HCl the precipitate does not dissolve but the sample changes its colour to yellow, typical of the samples of type A. This is accompanied by the change in the FIR spectrum [24]. The bands at 340 and 378 cm^{-1} disappear while a new band at 320 cm^{-1}, characteristic of Cl–Pd–Cl bridging structures [25,26] is present.

In the UV–Vis spectra recorded for solid samples B (Fig. 4) besides broad bands similar to these in sample A in the region of 380–410 nm, very intensive increase of the background at 800–900 nm appears. Similar spectroscopic effect has been observed during Pd/TiO_2 and Pd/SiO_2 catalyst preparation [27,28]. According to the authors, this increase of the background is due to the precipitation of palladium oxide or hydroxide on the TiO_2 or SiO_2 surface. Thus in $PdCl_2$ solution of low acidity (type B) due to basic properties of PVP hydrolysis of palladium complexes

takes place resulting in the formation of hydrated palladium oxide or hydroxide. This conclusion is confirmed by XPS analysis. In samples B, the palladium peak at $BE_{Pd\,3d_{5/2}} = 336.8$ eV very close to that observed for PdO_X/TiO_2 [27] and in good agreement with the values of binding energy recorded for PdO (336.3 eV) [29,30] was observed. On the other hand, in the case of samples A the value of binding energy equal to 337.5 eV, which is in good agreement with that characteristic of Pd–Cl has been detected.

3.1.2. PANI

PANI is a conjugated polymer whose repeating unit is presented in Scheme 1. This unit consists of y reduced and $(1 - y)$ oxidized units. The polymer can continuously change its oxidation state from the fully reduced ($y = 1$) to the fully oxidized ($y = 0$) one. Additionally, owing to basic properties (presence of amine (–NH–) and imine (=N–) groups), PANI undergoes protonation reactions easily with acids giving salts. Thus, PANI reacts readily in the redox as well as acid–base reactions. In the present studies, PANI in form of polyemeraldine ($y = 0.5$) has been used.

As has been already noticed, the procedures used to prepare series A and B of Pd/PANI samples has differed only in the HCl concentration in the $PdCl_2$–HCl–H_2O solution and in consequence in the type of Pd^{2+} complexes dominating in individual series. XPS (Table 1), FTIR (Fig. 5) and UV–Vis (Fig. 6) spectra show that different processes occur during doping of PANI in systems A and B. XPS data unequivocally show that in system A palladium is incorporated into PANI at the Pd^{2+} oxidation level ($BE_{Pd\,3d_{5/2}} = 337.7$ eV) while in samples B prepared in solution of low acidity two Pd states can be distinguished [22,31]: Pd^0 ($BE_{Pd\,3d_{5/2}} = 335.4$ eV) and Pd^{2+} ($BE_{Pd\,3d_{5/2}} = 337.7$ eV). The N 1s spectra of

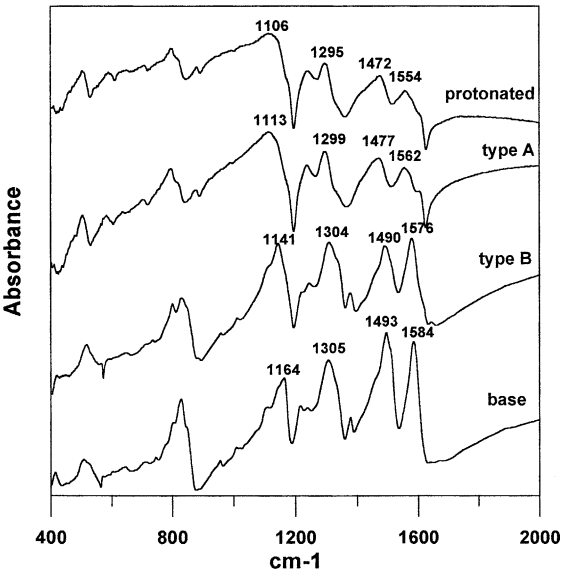

Fig. 5. FTIR spectra of PANI base, Pd/PANI samples of types A and B and PANI protonated with HCl.

both types of samples contain the components corresponding to imine (=N–, $BE_{N\,1s} = 398.3$ eV), amine (–NH–, $BE_{N\,1s} = 399.4$ eV) and charged nitrogen atoms ($–N^+–$, BE value higher than 400 eV). The doping of PANI in both systems is manifested by the decrease of the share of the peaks corresponding to =N– and increase of that of $–N^+–$. The changes are stronger for the sample A. Hence, in both systems the protonation process occurs but it proceeds to higher extent in system A. Protonation of PANI has also been confirmed by FTIR spectra (Fig. 5) of palladium-containing samples, which can be briefly described as follows:

- A new peak at 1141 cm^{-1} assigned to the doped PANI chain appears. This peak is characteristic of

Table 1
XPS data of PANI base and PANI doped in solutions A and B

Sample	N 1s						Pd 3d			
	=N–		–NH–		N^+		Pd^{2+}		Pd^0	
	BE (eV)	Share (%)	BE (eV)	Share (%)	BE (eV)	Share (%)	BE (eV)	Share (%)	BE (eV)	Share (%)
PANI	398.3	45	399.4	45.3	401.0, 402.9	9.7				
Sample A	398.6	16.2	399.3	57.3	400.6, 401.9	26.5	337.7, 343.1	100	–	
Sample B	398.3	31	399.4	49.9	400.6, 402.5	19.1	337.7, 343.0	80	335.4, 340.4	20

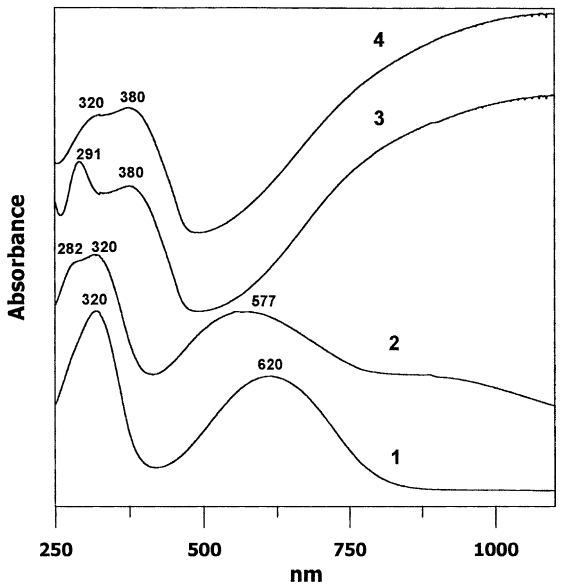

Fig. 6. UV–Vis spectra of films of PANI base (1), PANI doped in weakly acidic solution B (2) and in strongly acidic solution A (3), and PANI protonated with HCl (4).

PANI protonated with acids [32] as well as of ionic salts-doped PANI (pseudoprotonation effect) [33].

- The bands at 1584 cm^{-1} (N=Q=N stretching, Q — quinoid unit) and at 1493 cm^{-1} (N–B–N stretching, B — benzenoid unit) shift to lower frequencies. The shifts in frequencies of both bands are different for samples A and B. For the samples A (prepared in solution of high acidity) both bands distinctly shift to lower frequencies (Fig. 5). In samples B, the shift of N–B–N frequency is quite small, whereas N=Q=N frequency shifts distinctly.

This indicates that in the presence of neutral $[PdCl_2(H_2O)_2]$ complexes, imine nitrogen atoms are doped while amine ones remain almost unchanged. On the other hand, in $PdCl_2$ solution of high acidity both types of nitrogen groups take part in the doping process which proceeds via protonation. Cl^- as well as palladium ions in the form of $[HPdCl_4]^-$ are introduced as counterions. However, from the UV–Vis analysis the coordination of palladium ions by the nitrogen atoms in PANI cannot be excluded especially in solution A. The UV–Vis spectrum of sample A (Fig. 6) shows features characteristic of the protonated PANI, i.e. a strong peak at 380 nm and an increasing absorption extending into the NIR spectral region as well as the new peak at 291 nm. It can be postulated that this new peak is associated with the complexation of Pd^{2+} by the polymer [22]. As has been already mentioned, the complexation of Cu^{2+}, Ag^+ and Pd^{2+} by PANI has been reported in literature [6–8]. The UV–Vis spectrum of sample B is significantly different (Fig. 6). Features characteristic of protonation are barely visible, which is consistent with the XPS and FTIR results. The spectrum of sample B is different from that of starting PANI (Fig. 6) because two strongly overlapping peaks at 282 and 320 nm and a broad one centred at 577 nm are present. This type of spectrum is characteristic of partially oxidized PANI. Thus, during the doping in the $PdCl_2$ solution of low acidity partial oxidation of PANI chain (transformation of –NH– to =N– groups) [17,22] accompanied by the reduction of Pd^{2+} to Pd^0 detected by XPS analysis (Table 1) takes place. The effect of partial oxidation of PANI has also been confirmed by Raman spectra [31].

3.2. Catalytic properties

3.2.1. Morphology of catalysts surface

From the catalytic point of view, it was interesting to correlate the catalysts activity with the surface morphology of Pd/PVP and Pd/PANI samples. XRD and SEM analyses showed that this morphology and especially palladium dispersion was strongly dependent on the method of catalysts preparation [16,34].

Pd/PANI catalysts of series B, in which Pd^{2+} were reduced to Pd^0 (Table 3) during their synthesis were used in hydrogenation tests without any preliminary reduction. In contrast, pristine Pd/PANI samples of series A, and Pd/PVP of series A and B, which contained only Pd^{2+} did not exhibit catalytic activity and therefore it was necessary to reduce them before catalytic tests. Reduction was carried out at room temperature (2 h) with a 0.1 M solution of NaH_2PO_2. No change in polymer structure was observed (confirmed by IR, XRD). In case of Pd/PVP catalysts (series A and B), the reduction of Pd^{2+} was complete (Table 4) which was confirmed by XPS. In case of Pd/PANI (Table 2), reduction of Pd^{2+} ions was never complete (only ∼80–90%). It should be observed that even after additional treatment of Pd/PANI of

Table 2
PANI, series A of catalysts

Catalyst	Pd (wt.%)	Pd^0 (wt.%)	Pd^0/Pd (%)	Rate H_2 (10^{-5} mol/min per gram Pd^0)
PANI (1A)	1	0.83	83.0	0.24
PANI (2A)	2.5	2.40	96.3	0.23
PANI (3A)	4	3.80	95.2	0.34
PANI (4A)	6	5.80	96.2	0.37
PANI (5A)	10	9.40	94.0	0.37

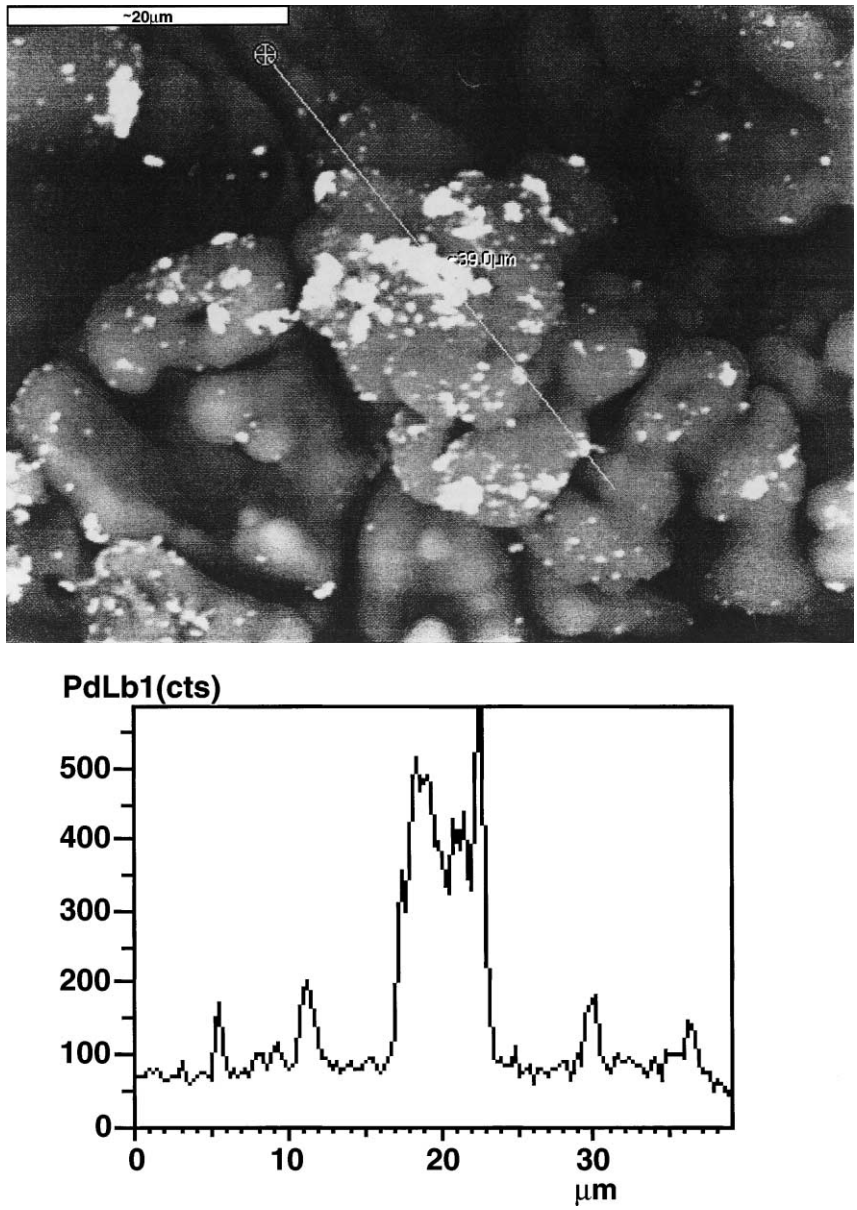

Fig. 7. SEM micrograph of Pd/PVP-series A, 4% Pd (magnification 1600).

series B, catalysts with NaH_2PO_2 solution no further reduction of Pd^{2+} took place.

SEM micrographs of Pd/PVP of type A and B catalysts, both containing about 4 wt.% Pd are presented in Figs. 7 and 8, respectively. In the former case, a very large irregularly shaped Pd agglomerates are seen, while in the latter the dispersion of palladium is very high. Fig. 9 shows the XRD spectra of PVP of samples A and B. In all X-ray patterns, the broad bands centred around $2\theta = 4.5$, 11 and 20° characteristic

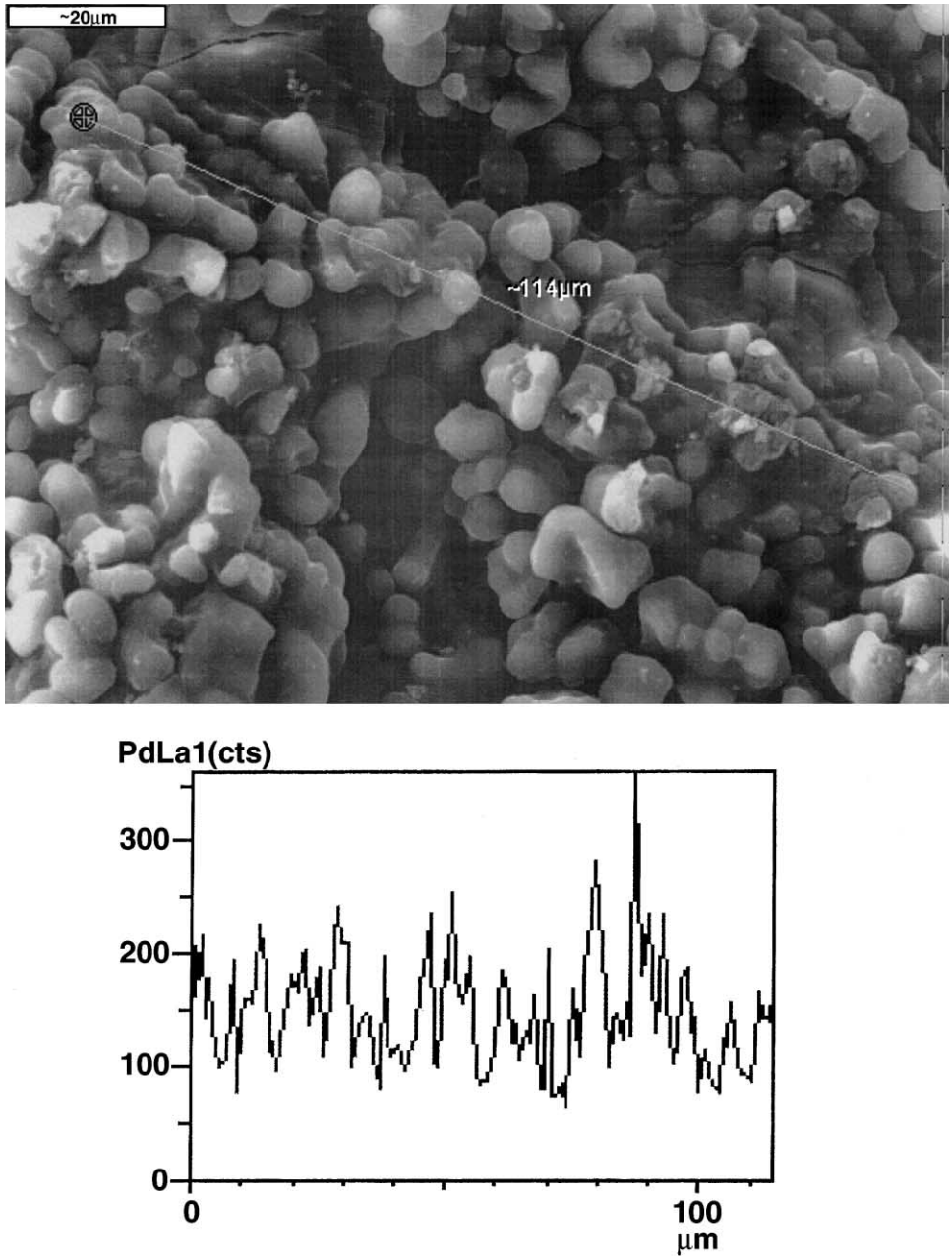

Fig. 8. SEM micrograph of Pd/PVP-series B, 4.14% Pd (magnification 1000).

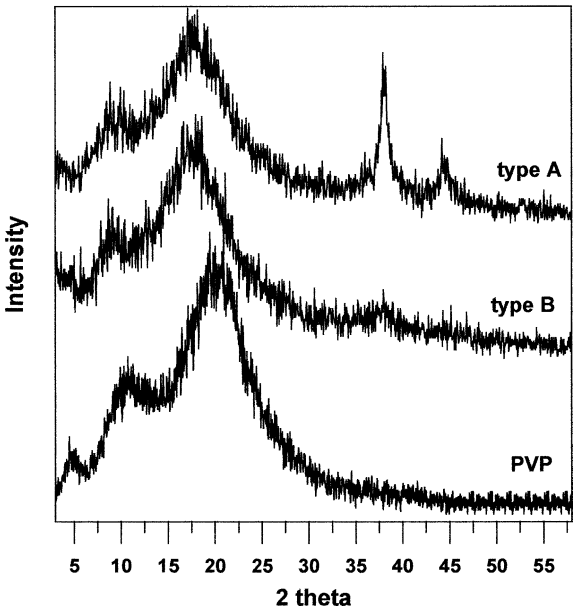

Fig. 9. XRD patterns of PVP and Pd/PVP sample of type A (4% Pd) and B (4.14% Pd).

of PVP support are present. It is seen that the reduction of sample A in which Pd^{2+} ions are mainly coordinated by nitrogen atoms leads to the formation of large crystalline agglomerates of Pd^0 observed as the intensive and broad peaks at $2\theta = 40.1$ and 46.6° (Fig. 9), although before catalyst reduction the dispersion of palladium ions was uniform. The effect of large Pd^0 aggregates formation is very similar to that observed for Pt–PVP system [35]. It has been shown [35] that Pt^0 particles produced after electrochemical reduction carried out in $[PtCl_6]^{2-}$–1 M HCl–PVP system were located in the bulk of the polymer. On the other side, Pt^0 produced in the same system but after chemical reduction (with hydrogen) appeared in the form of larger aggregates (~0.3 μm) located mainly on the PVP surface.

On the other hand, in Pd/PVP catalysts of series B in which as a result of hydrolysis palladium oxide (or hydroxide) was precipitated, Pd^0 formed after catalysts reduction was very uniformly distributed (Fig. 8) as line profile of Pd analysis showed. Fig. 9 shows that Pd^0 in this sample B appeared in the form of particles of size below the XRD detection limit. Hence, the nature of Pd^{2+}–PVP interactions and in consequence

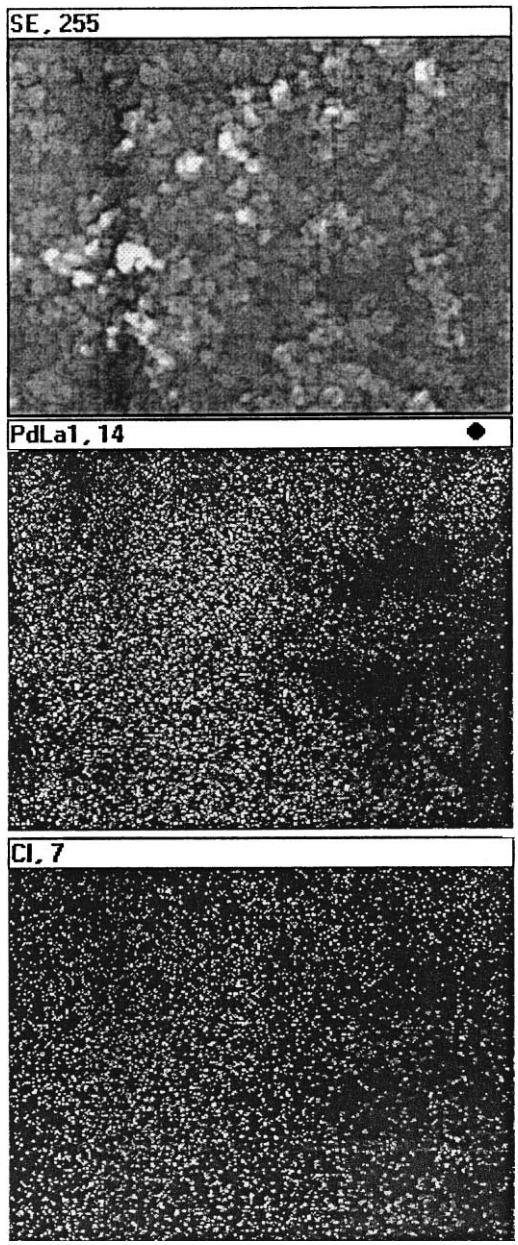

Fig. 10. SEM distribution of Cl and Pd, catalyst Pd/PANI (5A) containing 9.4% Pd^0 (magnification: ×4000).

the type of Pd^{2+}–polymer species formed strongly influenced the dispersion of Pd^0 in the final catalysts.

This observation is also true for Pd/PANI catalysts. As SEM micrograph shows (Fig. 10), after reduc-

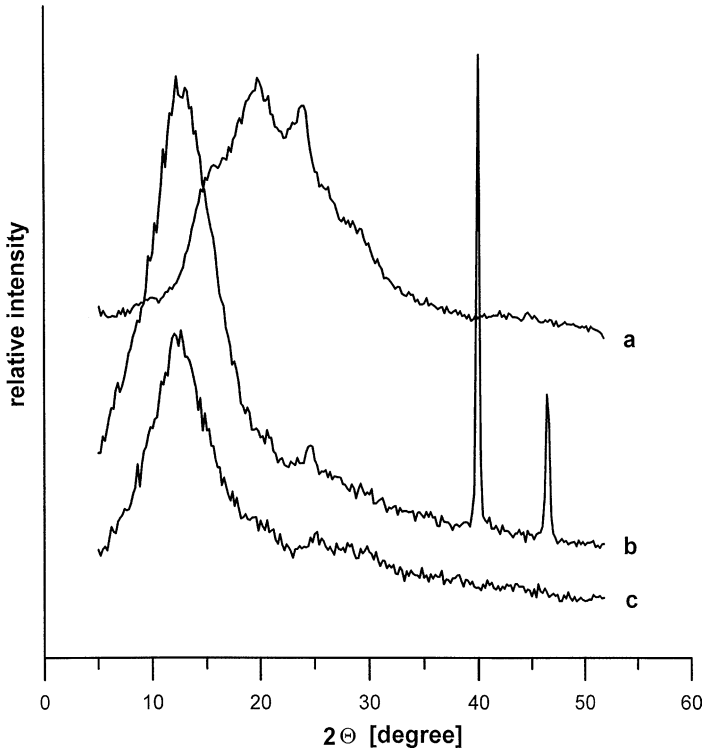

Fig. 11. X-ray diffraction patterns of: (a) PANI; (b) sample Pd/PANI (4B) containing 4.63% Pd^0; (c) sample Pd/PANI (4A) containing 5.8% Pd^0.

tion of samples A into which Pd^{2+} was introduced mainly via protonation in the form of counterions the dispersion of Pd^0 is very high and the size of Pd^0 particles is practically below the XRD detection limit (Fig. 11). Fig. 11 presents diffraction pattern of PANI base, samples A and B. In the X-ray spectrum of PANI base (Fig. 11, curve a), a broad 'halo' centred around $2\theta = 20^\circ$ is present. The diffractograms of PANI doped with palladium (Fig. 11, curves b and c) exhibited an intense peak at $2\theta = 14^\circ$ while no reflections assigned to the PANI-base structure are present. Such diffraction patterns consisting of a single "crystalline" peak suggest one-dimensional ordering in the PANI–palladium systems.

Surface morphology of Pd/PANI catalysts of series B prepared in $PdCl_2$ solution of low acidity (Figs. 11 and 12) was completely different [16]. In this system, Pd^0 was created during the catalysts preparation via reduction–oxidation process proceeding with the participation of the polymer chain. As the result of this type of interactions, crystalline Pd^0 particles (100–600 nm in size) were formed observed in XRD pattern (Fig. 11) as sharp and narrow peaks at $2\theta = 40.1$ and 46.6°. SEM micrograph typical for the Pd/PANI samples of series B is presented in Fig. 12. The distinct Pd particles in the form of white spots exhibiting high contrast against the support are seen. The regular, spherically shaped metal particles were quite uniformly dispersed over the PANI surface. According to our earlier observations [16] independently of Pd amount, the shape of all palladium particles were similar. With increasing content of Pd^0 in the catalysts, the density of palladium particles as well as their size increased.

Thus, results of SEM and XRD investigations indicate that conditions of catalysts preparation affected not only the mechanism of Pd^{2+}–polymers (PVP, PANI) interactions and hence the type of species formed but also the dispersion of Pd^0 in the final samples.

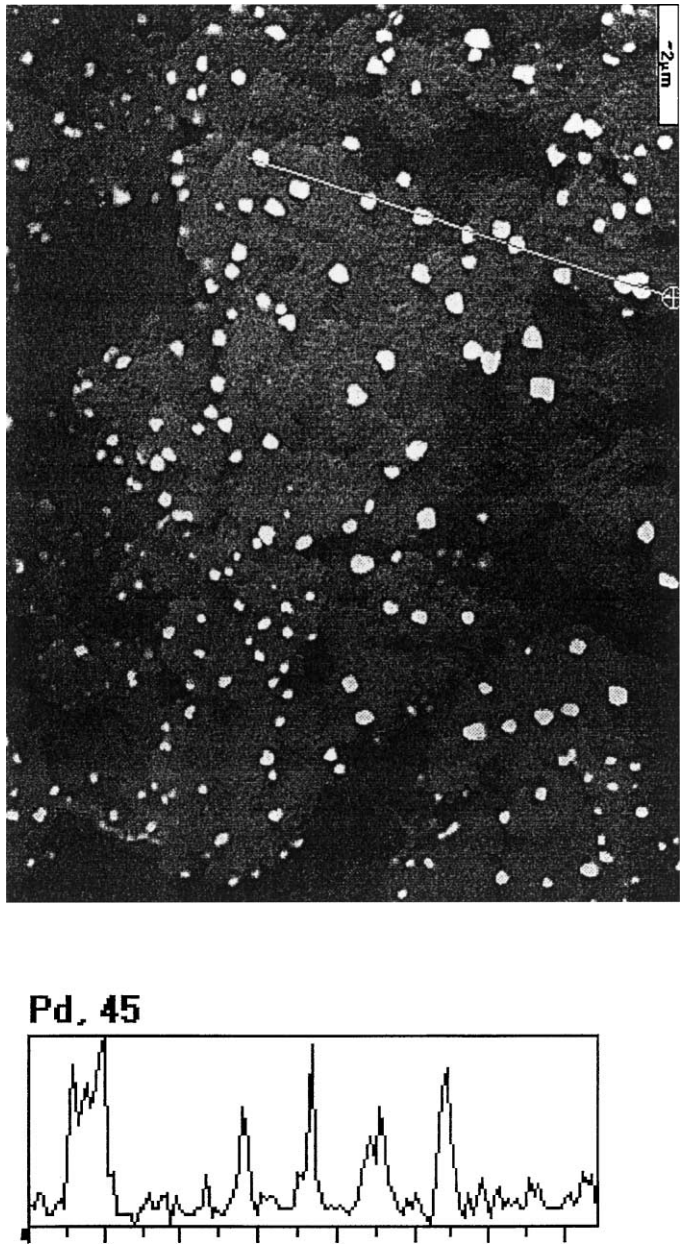

Fig. 12. SEM micrograph and X-ray line profile of Pd/PANI (4B) containing 4.63% Pd^0.

3.2.2. Catalytic activity

Catalytic ability of Pd/PVP and Pd/PANI samples containing 1–10 wt.% of Pd (Tables 2–4) was examined in hydrogenation of EAQ. As already noted, catalytic hydrogenation of EAQ is the key reaction in the anthraquinone method of H_2O_2 production (Scheme 2). However $EAQH_2$, the primary product of EAQ reduction is partly hydrogenated to different products, among which only H_4EAQH_2 is the desired one (Scheme 3) because it can participate in the oxi-

Table 3
PANI, series B of catalysts

Catalyst	Pd (wt.%)	Pd^0 (wt.%)	Pd^0/Pd (%)	Rate H_2 (10^{-5} mol/min per gram Pd^0)
PANI (1B)	1	0.93	93.5	0.21
PANI (2B)	2.5	2.05	82.2	0.19
PANI (3B)	4	3.32	82.9	0.23
PANI (4B)	6	4.63	77.2	0.17
PANI (5B)	10	8.32	83.2	0.09

Table 4
PVP, series B of catalysts

Catalyst	Pd^0 (wt.%)	Rate H_2 (10^{-5} mol/min per gram Pd^0)
PVP (1B)	0.80	1.19
PVP (2B)	2.20	0.95
PVP (3B)	2.96	1.09
PVP (4B)	4.14	1.13
PVP (5B)	5.80	1.05
PVP (6B)	8.00	1.00

dation reaction leading to H_2O_2 formation (similar to Scheme 2). Therefore, EAQ and H_4EAQ are termed "active quinones" while all other products formed (2-ethyloctahydroanthraquinone, 2-ethylanthrone, 2-ethyloxanthrone [11,36–38]), not capable of H_2O_2 formation are termed "degradation products". From technological point of view, the formation of low amount of degradation products is required.

It was interesting to study the effect of the type of polymer and the dispersion of Pd^0 on the course of EAQ hydrogenation and especially on the change of the amount of active quinones (EAQ, H_4EAQ). It was assumed in these investigations that SEM micrographs were representative for the entire surface of catalysts and that the total amount of palladium acting in hydrogenation is palladium detected by SEM method.

The course of EAQ hydrogenation was followed by measuring the volume of hydrogen consumed as a function of reaction time. From this correlation, the rate of hydrogenation expressed as the number of H_2 mol/min per gram of Pd^0 in catalysts was calculated. The values of initial rate of hydrogenation in the presence of Pd/PANI (series A and B) and Pd/PVP (series B) catalysts are presented in Tables 2–4. It should be observed that activity of Pd/PVP catalysts of series A, containing very large Pd^0 agglomerates (Fig. 7) was very low, the rate of hydrogen uptake was practically non-measurable.

From the data in Tables 2–4 it is evidently seen that within the whole contents of Pd in the samples, Pd/PVP catalysts exhibit distinctly higher activity. This activity is about 3–4 times higher than that over Pd/PANI catalysts. In the case of Pd/PVP catalysts, the rate of hydrogenation calculated per 1 g of Pd^0 is practically constant within the total range of Pd^0 contents (0.8–8 wt.% Pd). The same effect is observed for Pd/PANI catalysts of series A in which the dispersion of palladium is very high (Fig. 10). In series B of Pd/PANI catalysts, the rate of hydrogenation per 1 g

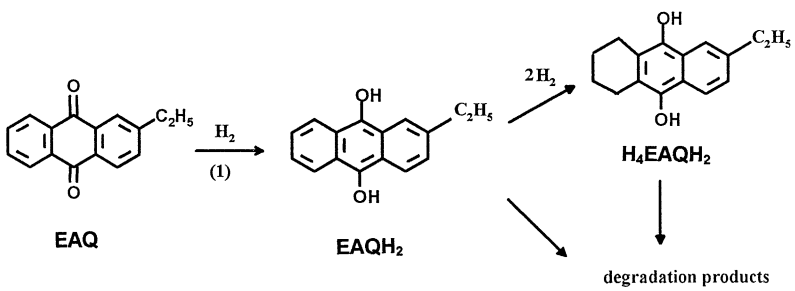

Scheme 3.

of Pd^0 decreases with increasing the content of Pd^0 in the catalysts. According to SEM and XRD analyses [16] with increasing the content of Pd^0 in this series increases the percentage contribution of larger palladium particles and as a consequence the rate decreases. At the lower contents of Pd^0 (up to ~2% Pd) in both series of Pd/PANI catalysts (A and B), the dispersion of palladium is similar [16] and in consequence the rates of hydrogenation are comparable.

In order to discuss selectivity effects, the catalytic results were expressed as a function of parameter β. This parameter represents the number of hydrogen moles consumed $\{n^t(H_2)\}$ per 1 mol of EAQ initially present in the reactor $\{n^0(EAQ)\}$:

$$\beta = \frac{n^t(H_2)}{n^0(EAQ)}$$

In the course of EAQ hydrogenation from the very beginning of the reaction up to $\beta = 1.2$–1.4, the reduction of EAQ to $EAQH_2$ is the main process [11,37]. After consumption of 1.2–1.4 mol of H_2 per 1 mol of EAQ, the hydrogenation of EAQ into $EAQH_2$ is almost complete [16,38]. At $\beta > 1.2$–1.4, usually the hydrogenation processes occur in which the primary product $EAQH_2$ is hydrogenated to H_4EAQH_2 and other side products (degradation products, Scheme 3). In the situation that from the beginning of hydrogenation only the reduction of EAQ to $EAQH_2$ proceeds, the highest possible number of H_2O_2 moles detected at $\beta = 1$ would be equal to the initial number of EAQ moles. This number of H_2O_2 moles has been assumed as 100%. In the case of selective hydrogenation of $EAQH_2$ to H_4EAQH_2 (active quinone) also 100% of H_2O_2 would be reached, but at values of β somewhat higher than 1. The change of $\%H_2O_2$ as a function of β is presented in Fig. 13. From the beginning of reaction, $\%H_2O_2$ distinctly increases as a result of EAQ to $EAQH_2$ reduction (main process) but at a certain value of β, higher than 1, it reaches the maximum value. In the second stage of hydrogenation, $\%H_2O_2$ decreases as a consequence of active quinone hydrogenation to degradation products. As Fig. 13 shows, in the presence of Pd/PVP and Pd/PANI catalysts (all contained about 4 wt.% Pd^0) still before reaching β value equal to 1, $EAQH_2$ has been consumed in undesired reactions, because in no case the value 100% H_2O_2 is reached. The maximum values of $\%H_2O_2$ have been reached at β higher than 1 thus indicating that in fact

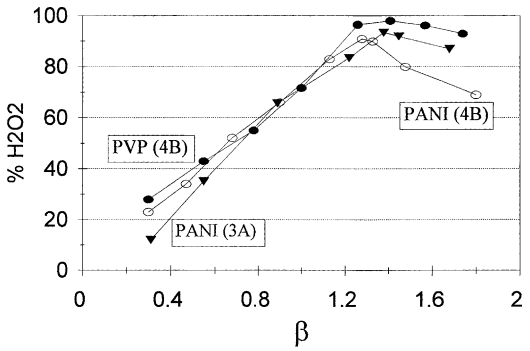

Fig. 13. Change of $\%H_2O_2$ as a function of β.

from the beginning of the reaction a part of hydrogen has been used for the formation products other than $EAQH_2$. The highest maximum value of $\%H_2O_2$ (98%) has been reached in the presence of Pd/PVP catalysts in which the dispersion of Pd^0 has been very high (Fig. 8), while the progress of undesired reactions has been the most intensive over Pd/PANI catalyst of series B (PANI (4B)) in which large Pd^0 agglomerates have been present (Fig. 12). Fig. 14 presents the change of the amount of H_4EAQH_2 formed (expressed as the mol% of all quinones) in the course of the reaction. In the presence of all catalysts, the formation of H_4EAQH_2 has been observed even at $\beta < 1$. At the value of $\beta > 1$, the highest amount of H_4EAQH_2 has formed over Pd/PANI catalysts of series B indicating that the process of aromatic ring hydrogenation proceeds most intensively over this catalyst. In the presence of this catalysts, the lowest was maximum value of $\%H_2O_2$ indicating that also the most intensively undesired reactions have proceeded.

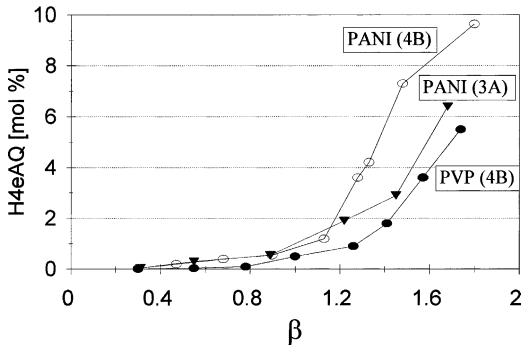

Fig. 14. Change of the amount of H_4EAQ as a function of β.

Hence, the presence of large Pd^0 crystalline particles facilitates aromatic ring hydrogenation as well as other undesired reactions in which degradation products are formed. This observation is in good agreement with our earlier results [34] which showed that in fact the size of Pd^0 agglomerates in Pd/PANI catalysts influenced the catalyst ability of $EAQH_2$ degradation.

It is evidently seen that the highest activity and simultaneously the lowest ability of $EAQH_2$ degradation exhibited palladium catalysts on PVP support. In this catalyst uniformly dispersed, very small Pd^0 particles were presumably present, created after reduction of palladium hydroxide (or oxide) precipitated on the polymers grains. On the other hand, Pd/PANI catalysts of series A in which also the high dispersion of palladium was detected exhibited lower activity. In this case, palladium ions in the form of the counterions $[HPdCl_4]^-$ or coordinatively bonded to the PANI acted as the precursors for Pd^0.

Hence, the best system for the catalytic hydrogenation of EAQ seems to be that prepared using PVP and $PdCl_2$ solution of type B.

4. Conclusions

1. Treatment of PVP and PANI with palladium chlorocomplexes present in $PdCl_2$–H_2O–HCl solutions makes it possible to prepare new palladium catalysts for liquid-phase hydrogenation of EAQ. Pd/PVP catalysts exhibit higher activity. The selectivity of hydrogenation process in their presence was also better than that detected for Pd/PANI samples. Surface morphology and especially the dispersion of palladium in Pd/PVP and Pd/PANI catalysts depend on the method of catalysts preparation. In particular, the dispersion of palladium is strongly influenced by the type of Pd^{2+}–polymers species formed which act as precursor for Pd^0. The type of such species is affected by the mechanism (protonation, coordination, oxidation–reduction reactions) of interactions between polymers and chlorocomplexes of palladium dominating in $PdCl_2$–H_2O–HCl solutions used for the catalysts preparation.
2. In the $PdCl_2$ solution containing predominantly anionic chlorocomplexes ($[PdCl_4]^{2-}$, $[PdCl_3(H_2O)]^-$, system A), the protonation (via acid–base reaction) and coordination of palladium ions with the participation of nitrogen atoms present in the polymers take place. In the case of PANI, protonation reaction is the dominating process and palladium ions are introduced mainly in the form of counterions. In the case of PVP formation of palladium complexes containing N as well as Cl ligands is an evident process.
3. In the $PdCl_2$ solution containing predominantly electrically neutral palladium chlorocomplex, i.e. $[PdCl_2(H_2O)_2]$ (system B) hydrolysis of this compound proceeds in the case of PVP and as the result palladium oxide (or hydroxide) precipitates on the polymer grains. In the case of PANI, the reduction–oxidation mechanism is involved resulting in the partial reduction of Pd^{2+} to Pd^0 accompanied by the oxidation of PANI chain (transformation of –NH– to =N–). However, it cannot be excluded that due to basic properties of PANI, the reduction–oxidation process is proceeded by hydrolysis of palladium chlorocomplex as well.
4. Various types of palladium–polymers species formed as the result of different nature of Pd^{2+}–polymers interactions influence the surface morphology and especially Pd^0 dispersion in the Pd/PVP and Pd/PANI catalysts.

In the situation when palladium ions are coordinated by nitrogen atoms as in case of Pd/PVP (system A), very large agglomerates of Pd^0 are formed after the catalysts reduction. Activity of this type of catalysts is very low (practically inactive). On the other hand, the precipitation of palladium hydroxide (or oxide) as a result of palladium complexes hydrolysis occurring due to basic properties of PVP leads to catalysts (series B) in which the dispersion of Pd^0 is very high. In consequence, the activity of this type of catalysts is high, higher than that of Pd/PANI catalysts (series A) in which also very small Pd^0 particles are present. However, in the latter case palladium ions, precursors for Pd^0 in the catalysts, are introduced mainly as counterions.

The other important effect, which according to many literature observation, affects catalysts activity is the swelling of the polymer support occurring in contact with the reaction medium (organic solvents). As a consequence, the particles of metal distributed inside of the polymer

mass become accessible for the reagents. It was found by SEM that swelling of PVP evidently proceeded after contacting it with ethanol. PVP grains observed in SEM were larger (expanded) after ethanol action than before. Hence, it cannot be excluded that the swelling of PVP occurring in contact with octanol-2 (solvent in hydrogenation reaction) influenced Pd/PVP activity.

In the case when palladium is introduced into the polymer (PANI) via the reduction–oxidation process, large crystalline Pd^0 particles (100–600 nm in size) are formed (Pd/PANI, series B).

5. The rate of the main process: hydrogenation of EAQ to $EAQH_2$ (Scheme 2) as well as other reactions leading to the formation of H_4EAQ and degradation products (Scheme 3) depend on the type of the polymer and the surface morphology of catalysts.

Presence of large crystalline Pd^0 particles in the catalyst (as in Pd/PANI catalysts, series B) accelerates reactions of aromatic ring hydrogenation as well as other processes leading to the formation of degradation products. Therefore, Pd/PVP samples of type B in which palladium hydroxide (or oxide) has served as precursor for Pd^0 seem to be the best catalysts for EAQ hydrogenation.

References

[1] O.S. Roszukina, M.W. Kliujev, Koord. Khim. 8 (1982) 188–200.
[2] L.N. Karklin, M.W. Kliujev, A.D. Pomagajlo, Kinet. Katal. 24 (1983) 408–412.
[3] D.V. Sokolski, A.K. Zharmagambetova, S.G. Mukhamedzhanova, E.A. Bekturov, S.E. Kudaibergenov, React. Kinet. Catal. Lett. 33 (2) (1987) 387–392.
[4] A.K. Zharmagambetova, I. Kurmanbayeva, T. Omarkulov, K. Kulazhanov, in: Proceedings of the Fourth European Congress on Catalysis, Rimini, September 1999, p. 262.
[5] H.G. Biederman, J. Obwander, K. Wichman, Z. Naturforsch. 27 (11) (1972) 1332–1335.
[6] A.Q. Zhang, C.Q. Cui, J.Y. Lee, F.C. Loh, J. Electrochem. Soc. 142 (1995) 1097–1104.
[7] D. Higuchi, T. Imoda, Hirao, Macromelucules 29 (1996) 8277.
[8] S. Kumar, R. Verma, B. Venkatarami, V.S. Raju, S. Gangadharan, Solvent Extr. Ion Exchange 13 (1995) 1097–1121.
[9] J.W. Sobczak, B. Lesiak, A. Jabłoński, A. Kosiński, W. Palczewska, Polish. J. Chem. 69 (1995) 1732–1737.
[10] S.W. Huang, K.G. Neoh, C.W. Shih, D.S. Lim, E.T. Kang, H.S. Han, K.L. Tan, Syn. Met. 96 (1998) 117–122.
[11] T. Ulmann, Encyclopedia of Industrial Chemistry, Vol. A3, VCH, Weinheim, 1989, pp. 443–466.
[12] C.S. Cronan, Chem. Eng. 6 (1959) 118–121.
[13] Ger. Offen DE 3,538,816 (1987).
[14] Y. Cao, A. Andreatta, A.J. Heeger, P. Smith, Polymer 30 (1989) 2313.
[15] J.G. Fraser, F.E. Bamish, W.A. MacBryde, Anal. Chem. 26 (1954) 495–503.
[16] A. Drelinkiewicz, M. Hasik, M. Kloc, J. Catal. 186 (1999) 123–133.
[17] A. Drelinkiewicz, M. Hasik, M. Kloc, Syn. Met. 102 (1999) 1307–1308.
[18] A. Drelinkiewicz, Bull. Pol. Acad. Sci. Ser. Chim. 39 (1991) 63–72.
[19] D. Thorburn Burns, R.K. Harlee, Anal. Chim. Acta 100 (1978) 563–569.
[20] H.A. Droll, B.P. Block, W.C. Renelius, J. Phys. Chem. 61 (1957) 1000.
[21] L. Rasmusen, Chr.K. Jorgensen, Acta Chem. Scand. 22 (1968) 2313–2325.
[22] A. Drelinkiewicz, M. Hasik, M. Choczyński, Mater. Res. Bull. 33 (1998) 739–762.
[23] N.S. Gill, R.H. Nutall, D.E. Scaife, D.W.A. Sharp, J. Inorg. Nucl. Chem. 18 (1961) 79–87.
[24] A. Drelinkiewicz, M. Hasik, S. Quillard, C. Paluszkiewicz, J. Mol. Struct. 511 (1999) 205–215.
[25] M. Pfeffer, P. Braunstein, J. Dehaud, Spectrochim. Acta A 30 (1974) 331–340.
[26] R.J.H. Clark, Ch. Williams, Inorg. Chem. 4 (1965) 350.
[27] P. Albers, K. Seibold, J. Chem. Soc., Faraday Trans. 86 (1990) 3671–3677.
[28] G.R. Tauszik, A. Marzi, R. Covini, React. Kinet. Catal. Lett. 7 (1977) 7–14.
[29] S.S. Chan, A.T. Bell, J. Catal. 89 (1984) 433–441.
[30] C.D. Wagner, Handbook of X-ray Photoelectron Spectroscopy, Perkin Elmer Phys. Elect. Dir., 1979.
[31] M. Hasik, A. Drelinkiewicz, M. Choczyński, S. Quillard, A. Proń, Syn. Met. 84 (1997) 93–94.
[32] J. Tang, X. Jing, B. Wang, F. Wang, Syn. Met. 24 (1998) 231.
[33] S.A. Chen, L.C. Lin, Macromolecules 28 (1995) 1239–1245.
[34] A. Drelinkiewicz, M. Hasik, M. Kloc, Catal. Lett. 64 (2000) 41–47.
[35] A. Kowal, K. Doblhofer, S. Krause, G. Weinberg, J. Appl. Electrochem. 17 (1987) 1246–1253.
[36] E. Santacesaria, M. Di Serio, R. Velotti, U. Leone, J. Mol. Catal. 94 (1994) 37–46.
[37] A. Drelinkiewicz, J. Mol. Catal. 75 (1992) 321–332.
[38] A. Drelinkiewicz, J. Mol. Catal. 101 (1995) 61–74.